Available online at www.sciencedirect.com
ScienceDirect
Journal of Magnetic Resonance 190 (2008) 33–42
JMR Journal of Magnetic Resonance
www.elsevier.com/locate/jmr

# The effect of the rotational angle on MR diffusion indices in nerves: Is the rms displacement of the slow-diffusing component a good measure of fiber orientation?

Amnon Bar-Shir, Yoram Cohen *

*School of Chemistry, The Raymond and Beverly Sackler Faculty of Exact Sciences, Tel Aviv University, Ramat Aviv, Tel Aviv 69978, Israel*

Received 16 July 2007; revised 11 October 2007
Available online 14 October 2007

**Abstract**

In recent years, much effort has been made to increase our ability to infer nerve fiber direction through the use of diffusion MR. The present study examines the effect of the rotational angle ($\alpha$), i.e. the angle between the diffusion sensitizing gradients and the main axis of the fibers in the nerves, on different NMR indices. The indices examined were the apparent diffusion coefficient (ADC), extracted from low $b$-values ($b_{max} \approx 1200$ s/mm$^2$), and the root mean square (rms) displacement of the fast and the slow-diffusing components extracted from high $b$-value q-space diffusion MR data. In addition, the effect of both the diffusion time and myelination was evaluated. We found that the most sensitive index to the rotational angle is the rms displacement of the slow-diffusing component extracted from the high b-value q-space diffusion MR experiment. For this component the rms displacement was nearly constant for $\alpha$ values ranging from $-10°$ to $+80°$ (where $\alpha = 0°$ is the $z$ direction), but it changed dramatically when diffusion was measured nearly perpendicular to the nerve fiber direction, i.e., for $\alpha = 90 \pm 10°$. The ADC and the rms displacement of the fast-diffusing component exhibited only gradual changes, with a maximal change at $\alpha = 45 \pm 15°$. The sensitivity of the rms displacement of the slow-diffusing component to the rotational angle was found to be higher at longer diffusion times and in mature fully myelinated nerves. The relevance of these observations for determining the fiber direction is briefly discussed.


*Keywords:* Nerves; Diffusion MRS; q-Space diffusion; Fiber direction; Apparent diffusion coefficient (ADC)

## 1. Introduction

Diffusion MR is a powerful method for studying neuronal tissues both *in vitro* and *in vivo*. Since the works of Le Bihan et al. [1] and Moseley et al. [2], diffusion MRI techniques have matured into a robust technique for characterizing structures and pathologies in the central nervous system (CNS) [3,4]. As early as 1990, Moseley et al. demonstrated by diffusion weighted imaging (DWI) that water diffusion is anisotropic in cat CNS [5]. This observed anisotropy was found to be much more prominent in white matter (WM) than in gray matter (GM) [5–7]. With the advent of the diffusion tensor imaging (DTI) technique by Basser et al. [8,9], water diffusion anisotropy was transformed into an important tool for studying both CNS connectivity and pathologies [10–12], despite the fact that even the origin of this observed anisotropy in neuronal tissues is still under debate [13].

Currently DTI, which is based on single-component analysis [8,9], exploits the observed anisotropy of water diffusion to tract fiber orientation by assuming that the fast-diffusing component coincides with the fiber's orientation [8–12,14–16]. Indeed, in recent years DTI techniques have been routinely used for whole-brain tractography in both animal models and in human subjects [8–12,14–16]. Although DTI is heavily used for studying WM structure and disorders, there are several issues concerning diffusion

* Corresponding author. Fax: +972 3 6407469.
*E-mail address:* ycohen@post.tau.ac.il (Y. Cohen).

1090-7807/$ - see front matter © 2007 Elsevier Inc. All rights reserved.
doi:10.1016/j.jmr.2007.10.007

in WM that are still not completely resolved. First, it was found that at sufficiently high diffusion weighting, the water signal decay in neuronal tissues, due to diffusion, is not mono-exponential [17,18]. Assignment of these components to different compartments is controversial [13]. Second, DTI has difficulties in characterizing crossing fibers that appear in one voxel [19]. Third, there is a need to reduce even further the relatively high uncertainty in defining the orientations of fibers [20]. These limitations prompted different research groups to develop new approaches to deal with these limitations. Some of these new approaches are HARDI (High Angular Resolution Diffusion Imaging [21]), DSI (Diffusion Spectrum Imaging [22]) and CHARMED (Composite Hindered and Restricted Model of Diffusion [23]).

The q-space approach, originally developed by Callaghan [24] and by Cory and Garroway [25], was subsequently proposed as a means to obtain structural information from high $b$-value (high q) diffusion MR data in neuronal tissues [26–31]. This approach was extended to MRI and was first used to study structures and pathologies in isolated organs using strong gradient systems [29,32]. Later, this approach was used on clinical MRI scanners to detect white matter associated disorders [30,33]. According to this method, one can obtain the displacement probability profile by Fourier transformation of the signal decay as a function of the reciprocal spatial vector $\mathbf{q}$. From the full-width at half-height (FWHH) of the displacement profile, one can extract the rms displacement of the diffusing component [24,25]. Therefore, with a sufficiently long diffusion time and a short diffusion gradient pulse, one can extract structural information on the compartment in which the diffusion takes place. These conditions need to be fulfilled since only under these conditions does the Fourier relationship between the signal decay as a function of q and the displacement probability function hold [24,25].

In a previous study, q-space analysis of NMR diffusion experiments, performed on microtubes with highly defined size and orientation [34], revealed high sensitivity of the diffraction patterns and the structural information obtained from the displacement distribution profiles on the rotational angle, $\alpha$. In that study, $\alpha$ was the angle between the diffusion gradient's direction and the main axis of the microtubes. These findings seem to suggest that the q-space analysis of heavily diffusion-weighted MR data can predict, with high sensitivity, the fiber orientation under investigation.

The purpose of this study was to examine the effect of the rotational angle, $\alpha$, on the root mean square (rms) displacement extracted from high $b$-value q-space diffusion experiments in nerve tissues. To this end, we tested the sensitivity of the two diffusing components that were extracted from this approach and the bulk apparent diffusion coefficient (ADC), obtained at low $b$-values, with respect to the rotational angle, $\alpha$, which reflects the fiber orientation relative to the diffusion gradient direction. In addition, we tested the influence of myelin and also evaluated the effect of the diffusion time on the extracted indices as a function of the rotational angle, $\alpha$.

## 2. Methods

Experiments were performed on formalin-fixed optic nerves of mature and newborn swine ($N = 3$ in each group). Briefly, a nerve sample of about 2 cm in length was immersed in Fluorinert and placed in a 5 mm NMR tube in such a way that the direction of its fibers was parallel to the $z$-direction, i.e., the $B_0$ direction (Fig. 1). NMR diffusion measurements were acquired using an 8.4T NMR spectrometer (Bruker, Germany) equipped with a micro5 gradient probe, capable of producing pulse gradients of up to 190 G cm$^{-1}$ in each of the three dimensions (i.e., $x$, $y$, and $z$). This probe is equipped with a BVT 3000 digital temperature control unit.

NMR diffusion experiments were conducted at 27 °C using the stimulated-echo diffusion sequence with the following parameters: TR/TE/$\delta$ = 2500/12.3/2 ms. Pulsed gradient strengths ($g$) were incremented from 0 to 160 G cm$^{-1}$ in 32 steps, resulting in a $q_{max}$ value of 1362 cm$^{-1}$. The separation between the gradient pulses, $\Delta$, was 7.0 and 100 ms for each rotational angle, $\alpha$, resulting in diffusion times of 6.3 and 99.3 ms, respectively. The rotational angle $\alpha$ was defined as the angle between the main axis of the magnet ($B_0$), which was parallel to the nerve fiber direction (i.e. the $z$-direction), and the direction of the gradient pulses in the NMR diffusion experiment (Fig. 1). Diffusion was measured for the following rotational angles ($\alpha$s): −10°, −5°, 0° ($z$-direction), 5°, 10°, 20°, 30°, 40°, 50°, 60°, 70°, 80°, 85°, 90° ($x$-direction), 95°, 100°, 180°, and 270°. Data for $\alpha = 90°$ and 270° or for $\alpha = 0°$ and 180° were also collected to verify whether background gradients are important. In these experiments we found that the contribution of the background gradients was negligible. The number of averages collected for each $q$-value in the NMR diffusion experiment was 40 and the total data set for each $\alpha$ was acquired in ~55 min. The signal-to-noise ratio (SNR) of a typical

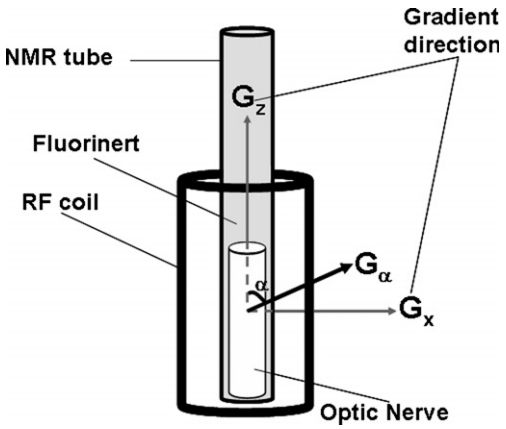


Fig. 1. The geometry of the sample and the definition of the rotational angle $\alpha$ i.e. the angle between the main axis of the nerve and the direction of the diffusion gradients.

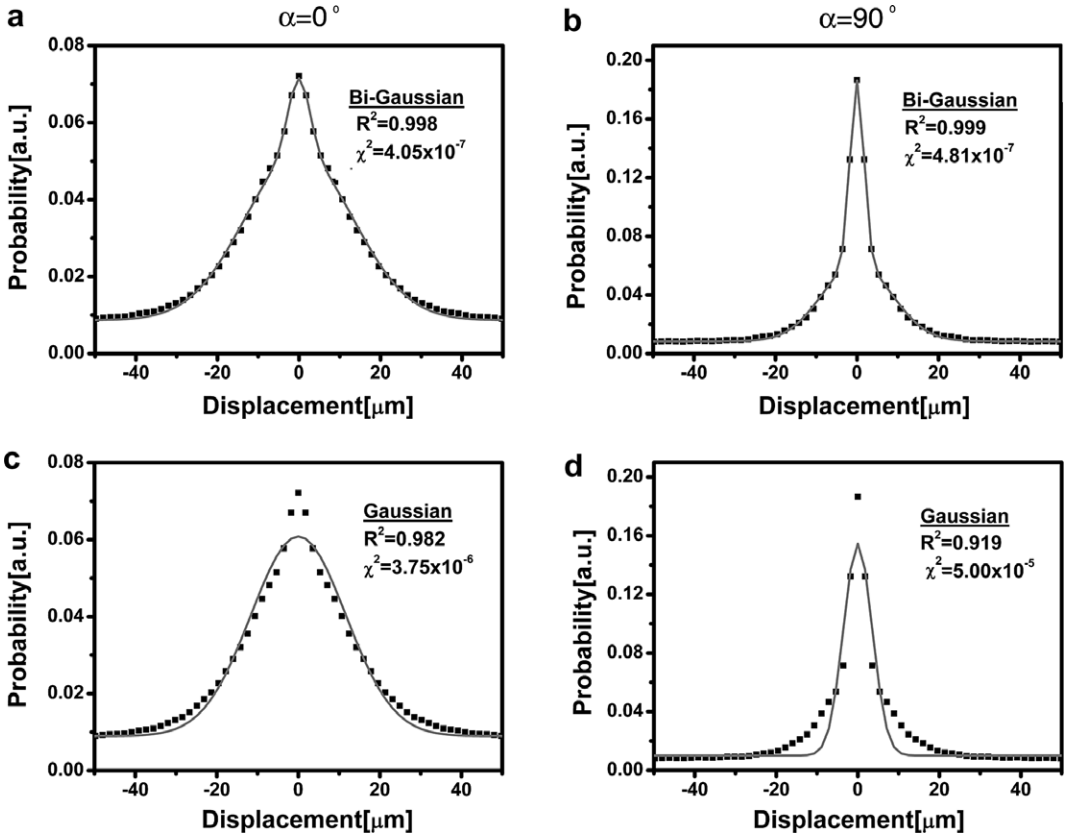


Fig. 2. The experimental displacement distribution profiles and the attempt to fit the experimental data with a single (c and d) and bi-Gaussian (a and b) functions for diffusion parallel ($\alpha = 0°$, a and c) and perpendicular ($\alpha = 90°$, b and d) to the fibers of the nerves.

diffusion $b = 0$ spectrum was about 11,000 and 4000 for mature and newborn optic nerves, respectively when $\Delta$ was 100 ms.

Displacement probability profiles were obtained by performing a Fourier transformation on the signal decay with respect to **q** and then fitting it with bi-Gaussian functions. A bi-Gaussian fit was performed since a single Gaussian function could not accurately fit the experimental data. For a bi-Gaussian fit, $R^2$ was generally above 0.998 and $\chi^2$ was less than $5 \times 10^{-7}$, respectively. In contrast, for a single Gaussian fit $R^2$ and $\chi^2$ were smaller than 0.991 and higher than $5 \times 10^{-6}$, respectively (see Fig. 2). From the FWHH of these profiles, we extracted the rms displacement of each diffusion component in the investigated nerves. The ADC values were extracted from the same data sets by linear fitting of the ln of the normalized signal decay (ln $(E/E_0)$) as a function of the $b$-values. In this case, three experimental points with b-values of 5, 617, and 1147 s/mm$^2$ (for $\Delta = 7$ ms) and 76, 684, and 1216 s/mm$^2$ (for $\Delta = 100$ ms) were used to calculate the bulk apparent diffusion coefficients (ADCs). These three points displayed mono-experimental signal decay and ln $(E/E_0)$, as a function of these $b$-values, gave a straight line with $R^2 > 0.999$. We also measured the $T1$-relaxation of the water peak in these nerves using an inversion recovery sequence.

After completion of the diffusion MRS experiments the nerves were fixed with glutaraldehyde solution, and then postfixed with 1% osmium tetra oxide ($OsO_4$) solution. The fixed samples were then dehydrated in graded ethanol solutions and embedded in Epon at 60 °C for 60 h. Two 1-μm sections were cut for each sample. The cut sections were stained with toluidine blue, a myelin staining reagent, and light and electron microscope images were taken from each sample.

## 3. Results

Fig. 3a and c show the ln of the normalized water signal decay (ln $(E/E_0)$) with respect to the reciprocal vector, **q**, at two different $\Delta s$ (i.e., 7 and 100 ms, respectively) for different representative $\alpha s$ in diffusion NMR experiments performed on a mature optic nerve. The displacement profiles shown in Fig. 3b and d were obtained by Fourier transformation of the data presented in Fig. 3a and c, respectively. These displacement profiles were fitted to bi-Gaussian functions, which enabled us to extract two diffusing components for the water in each nerve, i.e., slow- and fast-diffusing components. At $\alpha s$ between 0° and 20°, the changes in the experimental data are rather small for both diffusion times. However, one can see much more pronounced differences in the signal decays (Fig. 3a and c) and in the displacement profiles (Fig. 3b and d) when the rotational angle $\alpha$ was changed from 70° to 90°.

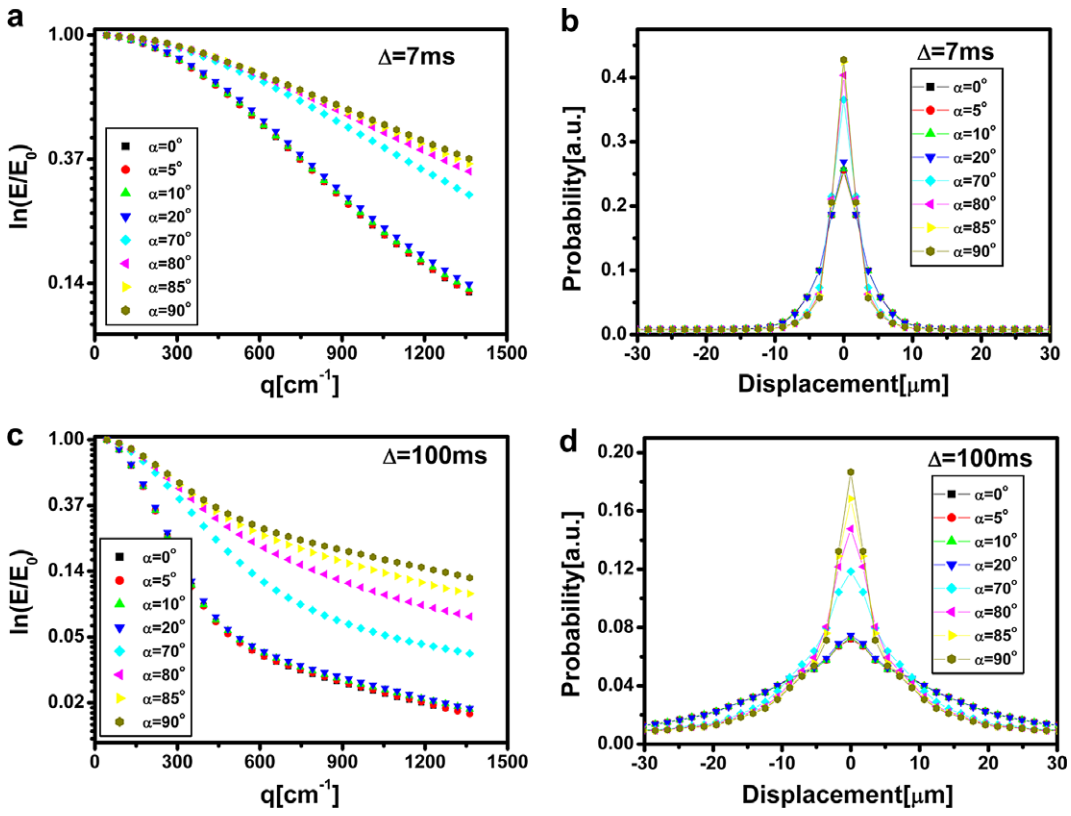


Fig. 3. The ln of the normalized water signal decay as a function of **q** in the mature optic nerve and as a function of different rotational angles ($\alpha s$) for (a) $\Delta = 7$ ms and (c) $\Delta = 100$ ms. The displacement distribution profiles (b and d) were obtained by Fourier transformation of the data shown in (a) and (c), respectively.

Fig. 4a and b depict the ln of the normalized water signal decay (ln $(E/E_0)$) with respect to the $b$-values for a mature optic nerve for $\Delta s$ of 7 and 100 ms, respectively. Here we analyzed only the low $b$-values range (i.e., $b_{max} \approx 1200$ s/mm$^2$), where signal decay is mono-exponential, as in cases of conventional DWI and DTI studies, which afford the bulk ADC. We used three low $b$-values to extract the ADC values for the different rotational angles ($\alpha s$). At both diffusion times (i.e., for $(\Delta - \delta/3) = 6.3$ or 99.3 ms), only small differences in the extracted ADC values were discerned when the rotational angles were varied from 70° to 90° or from 0° to 20°.

Fig. 5 shows the effect of the rotational angle ($\alpha$) on the rms displacements and ADC values, extracted from the NMR diffusion experiments, for a mature optic nerve for a $\Delta$ value of 100 ms. Fig. 5a and b depict the changes in the rms displacements of the slow- and fast-diffusing components obtained from the q-space analysis of the diffusion NMR data, respectively, whereas Fig. 5c shows the dependence of the ADC values on the rotational angle $\alpha$. These

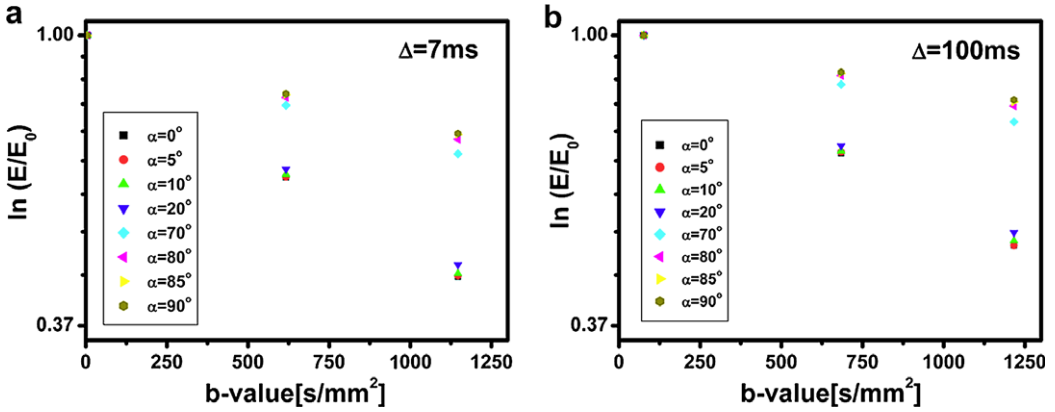


Fig. 4. The ln of the normalized signal decay as a function of low range $b$-values ($b < 1250$ s/mm$^2$) for different $\alpha s$ for (a) $\Delta = 7$ ms and (b) $\Delta = 100$ ms.

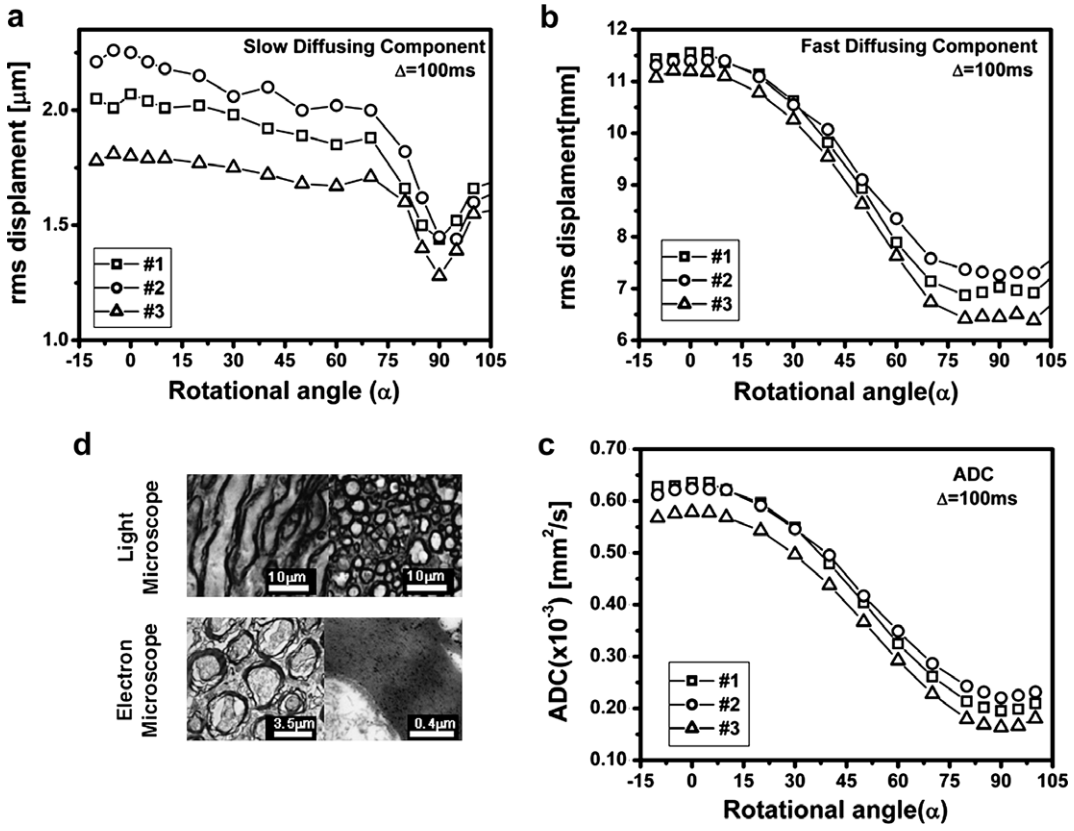


Fig. 5. Changes in the indices extracted from NMR diffusion experiments performed on three mature optic nerves with $\Delta = 100$ ms, as a function of the rotational angle, $\alpha$. (a and b) Show the changes in the rms displacements of the slow- and fast-diffusing components, respectively, extracted from the q-space analysis of the NMR diffusion experiments. (c) Depicts the changes in the ADC values extracted from the linear range of the signal decay ($b < 1250$ s/mm$^2$). (d) Shows light and electron microscope images of the investigated nerves.

figures show that the dependency of both the fast-diffusing component, extracted from the q-space analysis (Fig. 5b), and the bulk ADC values (Fig. 5c) on the rotational angles ($\alpha$s) is very similar. Moreover, the two indices do not change significantly when $\alpha$ is changed in the range of $90 \pm 10°$, i.e., when the diffusion is measured perpendicular to the main axis of the fibers. The same phenomenon is observed for $\alpha s$ in the range of $\alpha = 0 \pm 10°$, i.e., when diffusion is measured parallel to the main axis of the nerve. Interestingly, the behavior of the slow-diffusing component, extracted from the q-space analysis of the diffusion data, is quite different. Fig. 5a shows that the rms displacement values of the slow-diffusing components of the three optic nerves investigated remain nearly constant for $\alpha s$ in the range of $-10°$ to $+80°$, but change drastically when diffusion is measured nearly perpendicular to the long axis of the fibers, i.e., when $\alpha = 90 \pm 10°$. For $\alpha s$ from $-10°$ to $+80°$ the changes in the rms displacement values of the slow-diffusing component are relatively small.

Fig. 6 shows a data set run with the same parameters obtained for the three newborn optic nerves examined in this study. This set of data shows the same trends as those observed for the mature optic nerves (compare Figs. 5 and 6). However, the effect of the rotational angle on the diffusion indices extracted from the diffusion NMR experiments appears less dramatic, as compared with those of the mature nerves. Note that the main difference between mature and newborn optic nerves is the reduced amount of myelin in the latter [35]. This is clearly manifested in the light- and electron-microscope images of the mature and newborn optic nerves presented in Figs. 5d and 6d, respectively. Despite the difference in the tissue characteristics, and the reduced amount of myelin in the newborn optic nerve, the rms displacement of the slow-diffusing component is again the most sensitive index to the rotational angle $\alpha$. Here again, the rms displacement of the slow-diffusing component is nearly constant for $\alpha s$ in the range of $-10°$ to $+80°$ but changes dramatically for $\alpha = 90 \pm 10°$.

Fig. 7 presents the percentage changes in the extracted bulk ADC and in the rms displacement of the slow- and the fast-diffusing components, to quantify the sensitivity of different NMR diffusion indices to the rotational angle. These percentage changes for $\alpha s$ of $0 \pm 5°$ and $0 \pm 10°$ are relative to the values for $\alpha = 0°$; for 85–95° ($\alpha = 90 \pm 5°$) and 80–100° ($\alpha = 90 \pm 10°$), they are relative to the values of $\alpha = 90°$ for both types of optic nerves. From this figure, one can conclude that the most sensitive index for a fiber orientation near $\alpha = 90°$ is the rms displacement of the slow-diffusing component extracted from the q-space

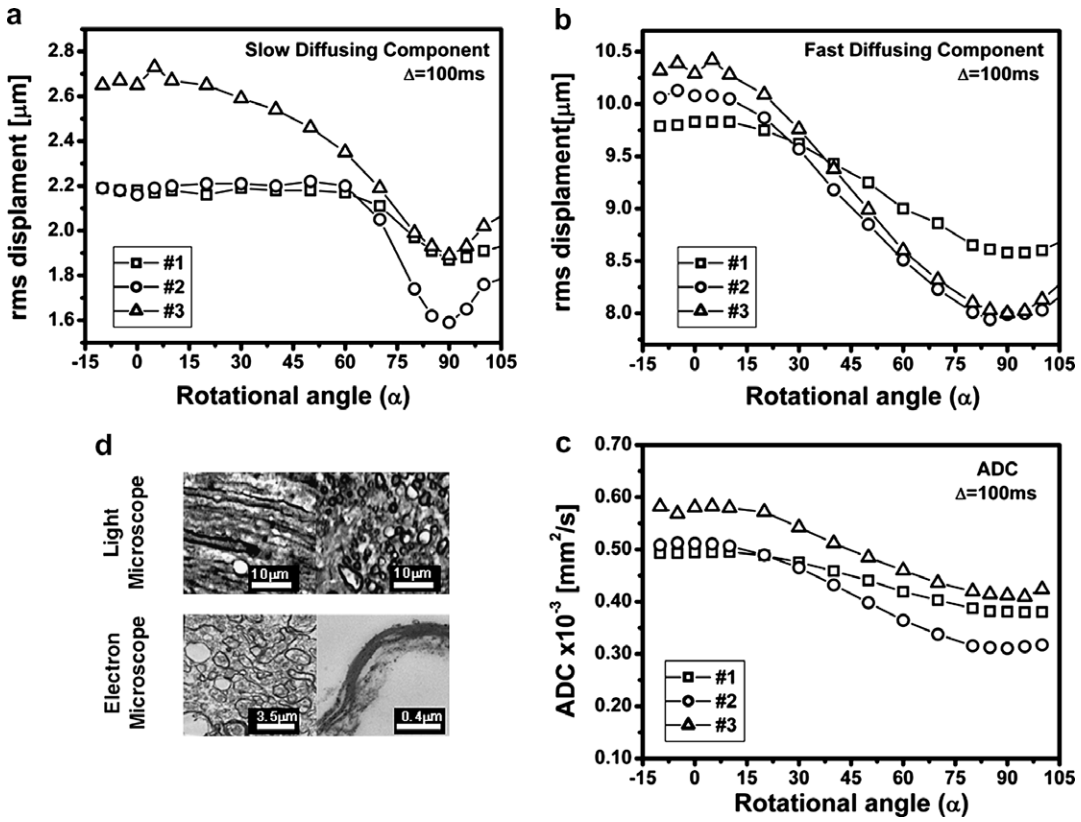


Fig. 6. The changes in the indices extracted from NMR diffusion experiments, performed on three newborn optic nerves with $\Delta = 100$ ms, as a function of the rotational angle, $\alpha$. (a and b) Present the changes in the rms displacements of the slow- and fast-diffusing components, as extracted from the q-space analysis of the NMR diffusion experiments. (c) Depicts the changes in the ADC values extracted from the linear range of the signal decay ($b < 1250\,\mathrm{s/mm^2}$). (d) Shows light and electron microscope images of the investigated nerves.

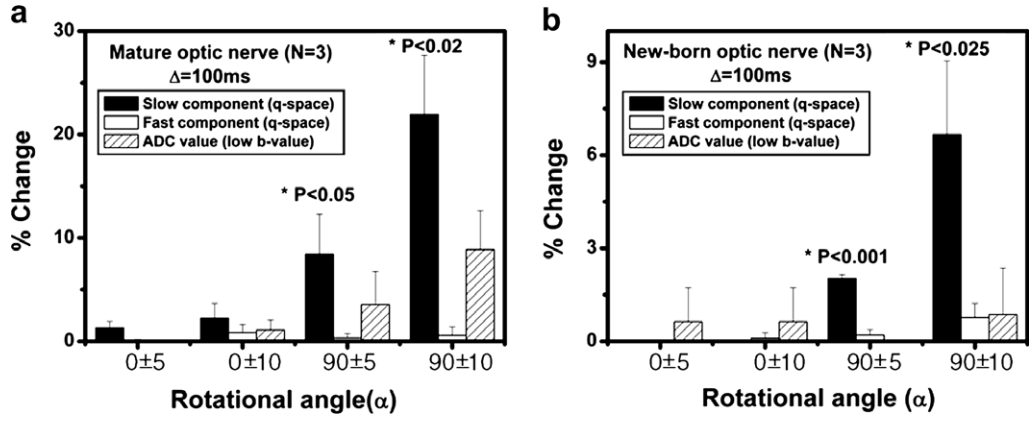


Fig. 7. The percentage change in the diffusion indices extracted from the NMR experiments as a function of the change in the rotational angle, $\alpha$, at a $\Delta$ of 100 ms for both (a) mature and (b) newborn optic nerves ($N = 3$ for each group). The values for $\alpha = 0 \pm 5°$ and $0 \pm 10°$ represent the percentage changes relative to the values for $\alpha° = 0°$, whereas the values for $\alpha = 90 \pm 5°$ and $90 \pm 10°$ represent the percentage changes relative to the values for $\alpha = 90°$. The $p$ values represent the statistical significance of the percentage changes as obtained by Student's $t$-test between the rms displacement of the slow component and the ADC values.

diffusion NMR experiments. For example, for the mature optic nerves at $\Delta = 100$ ms, we found the percentage change in the rms displacement of the slow and more restricted component to be $8 \pm 4\%$ in the 85–95° range, i.e., $\alpha = 90 \pm 5°$, and $22 \pm 6\%$ in the 80–100° range, i.e., $\alpha = 90 \pm 10°$, but insignificant for the fast-diffusing component. The ADC values for a mature optic nerve changed by $4 \pm 3\%$ and $9 \pm 4\%$ for $\alpha s$ from 85–95° and 80–100°, respectively, and showed nearly no change for $\alpha s$ of $0 \pm 5°$ and only $1.1 \pm 0.9\%$ change for $\alpha s$ of $0 \pm 10°$. Interestingly, both rms displacements of the slow and fast-diffusing components changed very little for $\alpha s$ of $0 \pm 10°$.

For the newborn optic nerves, the same trend was observed (Fig. 7b) but the differences were much less pronounced. The numerical values for the percentage changes in the three different indices studied are presented in Table 1.

We also examined the effect of the rotational angle on the extracted indices when the diffusion time was set to 6.3 ms. As we showed previously, a diffusion time of 6.3 ms is long enough to observe a significant restriction in the case of mature optic nerves, which have an average axon size of 1.1–1.3 μm [36]. Fig. 8 summarizes the observed percentage changes in the bulk ADC values and rms displacements of the fast- and slow-diffusing components when the diffusion time was set to 6.3 ms. As shown in this figure, although the differences between the diffusion indices extracted from the NMR experiments are less significant, and the percentage changes are lower for all rotational angles, the same patterns of behavior are observed for this short diffusion time and for both types of optic nerves. Here again, the most sensitive index is the rms displacement of the slow-diffusing component and for $\alpha s$ of $90 \pm 10°$. Note that the differences in the results obtained for $\Delta s$ of 7 and 100 ms do not arise from the $T1$-filtering effect of the signal. In $T1$ inversion recovery measurements performed on mature nerves, we observed only one component having a $T1$ value of $675 \pm 20$ ms.

## 4. Discussion

In the present study we examined the dependency of the rms displacements of the slow- and fast-diffusing components, extracted from high $b$-value q-space NMR diffusion experiments, on the rotational angle, $\alpha$. In addition, we investigated the influence of this parameter on the ADC values obtained from low b-value conventional diffusion MRS experiments. The dependency of the q-space rms displacements and the ADC obtained from conventional DWI was evaluated at two very different diffusion times and for both mature and newborn optic nerves. As demonstrated previously, at sufficient long diffusion times, i.e., longer than 6 ms, the slow-diffusing component mostly represents the restricted water (i.e., mostly intra-axonal and myelin water), whereas the fast-diffusing component mostly originates from water that diffuses more freely between the axons [35]. Since we have used a time to echo (TE) of 12.3 ms, which is relatively short, some contribution from myelin water cannot be ruled out a priori.

Avram et al. showed that the diffraction patterns, as well as the structural information obtained from q-space diffusion NMR experiments performed on microtubes, are sensitive to the rotational angle, $\alpha$ [34]. In this study, diffraction patterns were observed only when diffusion was measured nearly perpendicular to the long axis of the cylinders, i.e., when $\alpha = 90 \pm 5°$. These results motivated us to explore the sensitivity to the rotational angle $\alpha$ of the rms displacements of the slow- and fast-diffusing components extracted from q-space diffusion MRS in optic nerves. As a reference, we also evaluated the effects of $\alpha$

Table 1
The percentage changes of the ADC and the rms displacement of the fast- and slow-diffusing components for different rotational angle ranges for both mature and newborn optic nerves for $\Delta$ values of 7 and 100 ms.

| $\Delta$ (ms) | Diffusion indices | Mature optic nerve ($N = 3$) Rotational angle range[a,b] | | | | Newborn optic nerve ($N = 3$) Rotational angle range[a,b] | | | |
|---|---|---|---|---|---|---|---|---|---|
| | | $0 \pm 5°$ | $0 \pm 10°$ | $90 \pm 5°$ | $90 \pm 10°$ | $0 \pm 5°$ | $0 \pm 10°$ | $90 \pm 5°$ | $90 \pm 10°$ |
| 7 | % Changes in the rms displacement of the slow-diffusing component | $0 \pm 0$ | $1.5 \pm 0.1$ | $3 \pm 3$ | $8 \pm 4$ | $0 \pm 0$ | [c] | [c] | $3 \pm 1$ |
| | % Changes in the rms displacement of the fast-diffusing component | $0 \pm 0$ | $0.7 \pm 0.1$ | [c] | $2 \pm 2$ | $0 \pm 0$ | $0 \pm 0$ | [c] | $0.7 \pm 0.7$ |
| | % Changes in the ADC values | $0 \pm 0$ | $0.9 \pm 0.8$ | [c] | $5 \pm 3$ | $0 \pm 0$ | $0 \pm 0$ | $0 \pm 0$ | $2 \pm 1$ |
| 100 | % Changes in the rms displacement of the slow-diffusing component | $1.3 \pm 0.6$ | $2. \pm 1$ | $8 \pm 4$ | $22 \pm 6$ | $0 \pm 0$ | $0 \pm 0$ | $2.0 \pm 0.1$ | $7 \pm 2$ |
| | % Changes in the rms displacement of the fast-diffusing component | $0.1 \pm 0.1$ | $0.8 \pm 0.8$ | [c] | [c] | $0 \pm 0$ | [c] | $0.2 \pm 0.2$ | $0.8 \pm 0.5$ |
| | % Changes in the ADC values | $0 \pm 0$ | $1.1 \pm 0.9$ | $4 \pm 3$ | $9 \pm 4$ | [c] | [c] | $0 \pm 0$ | [c] |

[a] The values for $\alpha = 0 \pm 5°$ and $0 \pm 10°$ are relative to the values for $\alpha = 0°$.
[b] The values for $\alpha = 90 \pm 5°$ and $90 \pm 10°$ are relative to the values for $\alpha = 90°$.
[c] SD is higher than mean value.

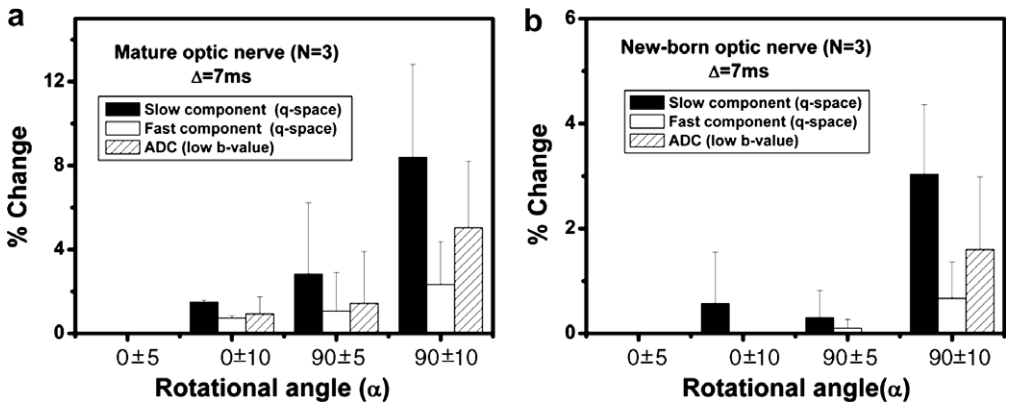


Fig. 8. The percentage change in the diffusion indices extracted from the NMR experiments as a function of the change in the rotational angle, $\alpha$, at a $\Delta$ of 7 ms for both (a) mature and (b) newborn optic nerves ($N = 3$ for each group). The values for $\alpha = 0 \pm 5°$ and $0 \pm 10°$ represent the percentage changes relative to the values for $\alpha = 0°$, whereas the values for $\alpha = 90 \pm 5°$ and $90 \pm 10°$ represent the percentage changes relative to the values for $\alpha = 90°$.

on the bulk ADC values obtained from low *b*-value diffusion NMR. Since diffraction patterns are generally not apparent in neuronal tissues [29–33,37], in contrast to what we found for uniform micro-cylinders [34], we focused on the rms displacement extracted from the FWHH of the displacement distribution profiles obtained. In addition, in a uniform micro-cylinders study [34], only a single Gaussian was needed to fit the data, whereas in the present study, bi-Gaussian functions were needed to fit the experimental data. Importantly, it was found that from the three indices examined in this study, the most sensitive one to the rotational angle, $\alpha$, is the rms displacement of the slow-diffusing component. For rms displacement of the slow-diffusing component, changing $\alpha$ from $-10°$ through $0°$ (parallel to the main axis of the fibers) to $+80°$ had nearly no effect, whereas a very dramatic effect was observed when the rotational angle was changed from 80° to 90° (perpendicular to the main axis of the fibers) and to 100° (i.e., for $\alpha = 90 \pm 10°$).

For rms displacement of the fast-diffusing component and the ADC values, the change in $\alpha$ had a gradual effect on the extracted values. The largest change in those diffusion indices occurred, in fact, for rotational angles between 20° and 70°. Interestingly, these angles do not coincide with actual directional characteristics of the sample, i.e., the direction of nerve fibers. The resemblance of the dependency of the ADC values and rms displacement of the fast-diffusing components implies that the ADC values extracted from low b-value diffusion NMR, although representing the average of all diffusing components in the investigated sample, carries mostly information on the fast-diffusing component. The ADC, being a weighted average of the fast- and the slow-diffusing components, showed an intermediate sensitivity to $\alpha$. Since the orientations of the investigated nerve fibers were well defined, it appears that the rms displacement of the slow-diffusing component, which represents mostly restricted water, is the most sensitive index for assessing fiber orientation. In addition, the results imply that measuring the diffusivity perpendicular to the long axis of the fibers may better predict of the fiber orientation, since the higher sensitivity to the rotational angle is, in fact, in the rms displacement of the slow-diffusing component obtained from the high *b*-values (high *q*) diffusion data.

Both tissue characteristics and experimental conditions used in the diffusion experiment may affect the diffusion results. The most important tissue characteristic in nerve seems to be the myelin, whereas the most crucial NMR experimental parameter is the diffusion time. Therefore, we evaluated the effect of diffusion time and myelination on the dependency of the different indices on the rotational angle $\alpha$. Indeed, we found that the sensitivity of the ADC and rms displacements of the fast- and slow-diffusing components on the rotational angle, $\alpha$, depends on the level of myelination and on the diffusion time used in the diffusion NMR experiment.

Interestingly, when newborn optic nerves, which are characterized by a much lower degree of myelination [29,35] (Figs. 5d and 6d) were used, the same patterns of behavior were observed for all three tested indices as in the mature nerve. However, in the poorly myelinated newborn nerves, the relative changes in the three investigated indices, when the rotational angle was varied, were significantly smaller, as can be concluded from comparing the data presented in Figs. 7 and 8. These results show that myelin does restrict water diffusion when diffusion is measured perpendicular to the main axis of the fibers. In more myelinated tissues the rms displacements are reduced, as compared with poorly myelinated nerves when diffusion is measured perpendicular to the direction of the fibers [29,38]. This result is in accordance with recent DTI studies performed on shiverer mice and q-space diffusion MRI of myelin-deficient rat spinal cord [38–40]. Indeed, for all cases in our study, the rms displacement of the slow-diffusing component, extracted from the q-space analysis of the high *b*-value diffusion NMR experiment, showed a very strong dependence on the rotational angle for $\alpha = 90 \pm 10°$.

For optic nerves, we previously showed that considerable restriction is observed at a diffusion time of about 6.3 ms or more [35]. Therefore, we expected that even for

a diffusion time as short as 6.3 ms, the percentage change for an $\alpha$ value of about 90° will be maximal for the rms displacement of the slow-diffusing component, as we indeed observed. As expected, at $\Delta = 7$ ms the difference in the percentage change of the rms displacement of the slow diffusing component for $\alpha = 90 \pm 10°$ is less affected by the degree of myelination. For $\Delta = 100$ ms these differences are much more dramatic, as one can conclude by comparing the results presented in Figs. 7 and 8 and in Table 1. Taken together, these results indicate that the rms displacement of the slow-diffusing component is the best index for determining fiber orientation. Therefore, it may well be that one should use the rms displacement of the slow-diffusing component obtained from heavily diffusion weighted MR data to tract fiber orientation. Note, however, that obtaining such diffusion data with the appropriate SNR may be time consuming, which in turn, may limit the applicability of this approach.

## 5. Conclusion

This study demonstrates that from all three indices investigated, the rms displacement of the slow-diffusing component, extracted from q-space diffusion NMR, exhibits the most significant dependence on the rotational angle, $\alpha$. We found that the rms displacement of the restricted component is nearly constant for $\alpha$s in the range of $-10°$ to $+80°$ but changes dramatically when $\alpha$ is $90 \pm 10°$. This phenomenon was found for both mature (myelinated) and newborn (poorly myelinated) fixed optic nerves and for short ($\Delta = 7$ ms) and long ($\Delta = 100$ ms) diffusion times. These findings imply that the rms displacement of the slow-diffusing component, as extracted from q-space diffusion NMR, is the best predictor for restriction and fiber direction. This finding may have implications concerning determination of fiber orientation by using diffusion NMR methodologies.

## Acknowledgments

This research was funded by ISRAEL SCIENCE FOUNDATION (ISF) Grant No. 522/03 and United States–Israel Binational Science Foundation (BSF) Grant No. 2003/353.

## References

[1] D. Le Bihan, E. Breton, D. Lallemand, P. Grenier, E. Cabanis, M. Laval-Jeantet, MR Imaging of intravoxel incoherent motions: application to diffusion and perfusion in neurological disorders, Radiology 161 (1986) 401–407.

[2] M.E. Moseley, Y. Cohen, J. Mintorovitch, L. Chileuitt, H. Shimizu, J. Kucharczyk, M.F. Wendland, P.R. Weinstein, Early detection of regional cerebral ischemia in cats: comparison of diffusion- and T2-weighted MRI and spectroscopy, Magn. Reson. Med. 14 (1990) 330–346.

[3] E.D. Schwartz, D.B. Hackney, Diffusion weighted MRI and the evaluation of spinal cord axonal integrity following injury and treatment, Exp. Neurology 184 (2003) 570–589.

[4] P.W. Schaefer, P.E. Grant, R.G. Gonzalez, Diffusion-weighted MR imaging of the brain, Radiology 217 (2000) 331–345.

[5] M.E. Moseley, Y. Cohen, J. KucharczykJ, J. Mintorovitch, H.S. Asgari, M.F. Wendland, J. Tsuruda, D. Norman, Diffusion-weighted MR imaging of anisotropic water diffusion in cat central nervous system, Radiology 176 (1990) 39–45.

[6] M.E. Moseley, J. Kucharczyk, H.S. Asgari, D. Norman, Anisotropy in diffusion-weighted MRI, Magn. Reson. Med. 19 (1991) 321–326.

[7] T.L. Chenevert, J.A. Brunberg, J.G. Pipe, Anisotropic diffusion in human white matter: demonstration with MR techniques in vivo, Radiology 177 (1990) 401–405.

[8] P.J. Basser, J. Mattiello, D. Le Bihan, MR diffusion tensor spectroscopy and imaging, Biophys. J. 66 (1994) 259–267.

[9] C. Pierpaoli, P.J. Basser, Toward a quantitative assessment of diffusion anisotropy, Magn. Reson. Med. 36 (1996) 893–906.

[10] D. Le Bihan, J.F. Mangin, C. Poupon, C.A. Clark, S. Pappata, N. Molko, H. Chabrait, Diffusion tensor imaging: concepts and applications, J. Magn. Reson. Imaging 13 (2001) 534–546.

[11] P.J. Basser, D.K. Jones, Diffusion-tensor MRI: theory, experimental design and data analysis- a technical review, NMR Biomed. 15 (2002) 456–467.

[12] S. Mori, P.C.M. van Zijl, Fiber tracking: principles and strategies, NMR Biomed. 15 (2002) 468–480.

[13] C. Beaulieu, The basis of anisotropic diffusion imaging in the nervous system, NMR Biomed. 15 (2002) 435–455.

[14] P.J. Basser, S. Pajevic, C. Pierpaoli, J. Duda, A. Aldroubi, In vivo fiber tractography using DT-MRI data, Magn. Reson. Med. 44 (2000) 625–632.

[15] J. Zhang, P.C.M. van Zijl, S. Mori, Three-dimensional diffusion tensor magnetic resonance microimaging of adult mouse brain and hippocampus, Neuroimage 15 (2002) 892–901.

[16] J. Zhang, L. Richards, P. Yarowsky, H. Huang, P.C.M. van Zijl, S. Mori, Three-dimensional anatomical characterization of the developing mouse brain by diffusion tensor microimaging, Neuroimage 20 (2003) 1639–1648.

[17] T. Niendorf, R.M. Dijkhuizen, D.G. Norris, M. Van Lookeren-Campagne, K. Nicolay, Bi-exponential diffusion attenuation curves in various states of brain tissue. The implications for diffusion-weighted imaging, Magn. Reson. Med. 36 (1996) 847–857.

[18] Y. Assaf, Y. Cohen, Non-mono-exponential attenuation of water and *N*-acetyl aspartate signals due to diffusion in brain tissue, J. Magn. Reson. 131 (1998) 69–85.

[19] W. Zhan, E.A. Stein, Y. Yang, Mapping the orientation of intravoxel crossing fibers based on phase information of diffusion circular spectrum, Neuroimage 23 (2004) 1358–1369.

[20] Y. Assaf, P.J. Basser, Composite hindered and restricted model of diffusion (CHARMED) MR imaging of the human brain, Neuroimage 27 (2005) 48–58.

[21] L.E. Frank, Characterization of anisotropy in high angular resolution diffusion-weighted MRI, Magn. Reson. Med. 47 (2002) 1083–1099.

[22] C.P. Lin, V.J. Wedeen, J.H. Chen, C. Yao, W.Y. Tseng, Validation of diffusion spectrum magnetic resonance imaging with manganese-enhanced rat optic tracts and ex vivo phantoms, Neuroimage 19 (2003) 482–495.

[23] Y. Assaf, G.K. Rohde, R.Z. Freidlin, P.J. Basser, A new modeling and experimental framework to characterize hindered and restricted water diffusion in brain white matter, Magn. Reson. Med. 52 (2004) 965–978.

[24] P.T. Callaghan, D. MacGowan, K.J. Packer, F.O. Zelaya, High resolution q-space imaging in porous materials, J. Magn. Reson. 90 (1990) 177–182.

[25] D.G. Cory, A.N. Garroway, Measurement of translational displacement probabilities by NMR-an indicator of compartmentation, Magn. Reson. Med. 14 (1990) 435–444.

[26] M.D. King, J. Houseman, S.A. Roussel, N. van Bruggen, S.R. Williams, D.G. Gadian, q-Space imaging of the brain, Magn. Reson. Med. 32 (1994) 707–713.

[27] M.D. King, J. Houseman, D.G. Gadian, A. Connelly, Localized q-space imaging of the mouse brain, Magn. Reson. Med. 38 (1997) 930–937.
[28] Y. Assaf, Y. Cohen, Assignment of the water slow diffusing component in CNS using q-space diffusion MRS: implications to fiber tract imaging, Magn. Reson. Med. 43 (2000) 191–199.
[29] Y. Assaf, A. Mayk, Y. Cohen, Displacement imaging of spinal cord using q-space diffusion weighted MRI, Magn. Reson. Med. 44 (2000) 713–722.
[30] Y. Cohen, Y. Assaf, High b-value q-space analyzed diffusion-weighted MRS and MRI in neuronal tissues—a technical review, NMR Biomed. 15 (2002) 516–542.
[31] C-L. Chin, F.W. Wehrli, Y. Fan, S.N. Hwang, E.D. Schwartz, J. Nissanov, D.B. Hackney, Assessment of axonal fiber tract architecture in excised rat spinal cord by localized NMR q-space imaging: simulations and experimental studies, Magn. Reson. Med. 52 (2004) 733–740.
[32] I.E. Biton, A. Mayk, D. Kidron, Y. Assaf, Y. Cohen, Improved detectability of experimental allergic encephalomyelitis in excised swine spinal cords by high *b*-value q-space DWI, Exp. Neurol. 195 (2005) 446–457.
[33] Y. Assaf, D. Ben-Bashat, J. Chapman, S. Peled, I.E. Biton, M. Kafri, Y. Segev, T. Hendler, A.D. Korczyn, M. Graif, Y. Cohen, High *b*-value q-space analyzed diffusion weighted MRI: application to multiple sclerosis, Magn. Reson. Med. 47 (2002) 115–126.
[34] L. Avram, Y. Assaf, Y. Cohen, The effect of rotational angle and experimental indices on the diffraction patterns and micro-structural information obtained from q-space diffusion NMR: implication for diffusion in white matter fibers, J. Magn. Reson. 169 (2004) 30–38.
[35] R.J. Colello, U. Pott, M.E. Schwab, The role of oligodendrocytes and myelin on axon maturation in the developing rat retinofugal pathway, J. Neurosci. 14 (1994) 2594–2605.
[36] A. Bar-Shir, Y. Cohen, High *b*-value q-space diffusion MRS of nerves: structural information and comparison with histological evidence, NMR Biomed. 20 (2007), on-line see:. doi:10.1002/nbm.1175.
[37] S. Peled, D.G. Cory, S.A. Raymond, D.A. Krischner, F.A. Jolez, Water diffusion, T2, and compartmentation in frog sciatic nerve, Magn. Reson. Med. 42 (1999) 911–918.
[38] I.E. Biton, I.D. Duncan, Y. Cohen, High *b*-value q-space diffusion MRI in myelin-deficient rat spinal cords, Magn. Reson. Imaging 24 (2006) 161–166.
[39] J.M. Tsyka, C. Readhead, E.L. Bearer, R.G. Paulter, R.E. Jacobs, Statistical diffusion tensor histology reveals regional dysmyelination effects in the shiverer mouse mutant, NeuroImage 29 (2006) 1058–1065.
[40] G. Nair, Y. Tamahashi, H.P. Low, S. Billings-Gagliardi, W.J. Schwartz, T.Q. Duong, Myelination and long diffusion time alter diffusion-tensor-imaging contrast in myelin-deficient shiverer mice, NeuroImage 28 (2005) 165–174.